

## **Recycler: an algorithm for detecting plasmids from de novo assembly graphs**

Roye Rozov<sup>1</sup>, Aya Brown Kav<sup>4</sup>, David Bogumil<sup>4</sup>, Eran Halperin<sup>1,2,3\*</sup>, Itzhak Mizrahi<sup>4</sup>, Ron Shamir<sup>1</sup>

<sup>1</sup> Blavatnik School of Computer Science, Tel-Aviv University, Tel Aviv, Israel

<sup>2</sup> Molecular Microbiology and Biotechnology Department, Tel-Aviv University, Tel Aviv, Israel

<sup>3</sup> International Computer Science Institute, Berkeley, CA, USA

<sup>4</sup> The Department of Life Sciences & the National Institute for Biotechnology in the Negev, Ben-Gurion University of the Negev, Beer-Sheva, Israel

\* corresponding author, [heran@icsi.berkeley.edu](mailto:heran@icsi.berkeley.edu)

### **Abstract**

Plasmids have important roles in antibiotic resistance and in affecting production of metabolites used in industrial and agricultural applications. However, their extraction through deep sequencing remains challenging, in spite of rapid drops in cost and throughput increases for sequencing. Here, we attempt to ameliorate this situation by introducing a new plasmid-specific assembly algorithm, leveraging assembly graphs provided by a conventional de novo assembler and alignments of paired-end reads to assembled graph nodes. We introduce the first tool for this task, called Recycler, and demonstrate its merits in comparison with extant approaches. We show that Recycler greatly increases the number of true plasmids recovered while remaining highly accurate. On simulated plasmidomes, Recycler recovered 5-14% more true plasmids compared to extant methods, and overall precision of about 90%. We validate these results on real data, by comparison against available reference sequences and quantifying annotation of predicted ORFs. All 12 of Recycler's outputs on isolate samples matched known plasmids or phages, and had alignments having at least 97% identity over at least 99% of the reported reference sequence lengths. For the two *E. Coli* strains examined, most known plasmid sequences were recovered, while in both cases additional plasmids only known to be present in different hosts were found. Recycler also generated plasmids in high agreement with known annotation on real plasmidome data. Moreover, 6 of 8 plasmids previously validated by PCR were completely recovered. Recycler is available at <http://github.com/Shamir-Lab/Recycler>

### **Introduction**

Plasmids are extra-chromosomal DNA segments carried by bacterial hosts. They are usually shorter than host chromosomes, circular, and encode nonessential genes. These genes are responsible for either plasmid-specific roles such as self-replication and transfer, or context-specific roles that can be beneficial or harmful to the host depending on its environment. Along with viruses and transposable elements, plasmids are members of the group termed mobile genetic elements [1] as they transmit genes and their selectable functions between microbial genomes. Plasmids play a central role in horizontal gene transfer [2], and thus genome innovation and plasticity - fundamental forces in microbial evolution.

Much interest has recently arisen for plasmid extraction and characterization, in particular because of their known roles in antibiotic resistance and in increasing metabolic outputs of agricultural or industrial byproducts. For instance, antibacterial resistance genes encoded on plasmids have long been known as a major issue for human health in clinical practice [3], but are also one of today's standard tools in microbiology and genetics when used to select for specific cells [4]. In order to derive plasmid sequences (which may be known or novel), one may choose from the following approaches: sequence already isolated microbes with their residing plasmids, sequence the overall microbial community of genomes (termed metagenome) from some environment, or, as was recently described, sequence only the overall plasmid fraction from a given environment (termed plasmidome) [5],[6]. The first technique obtains a mixture of chromosomal and plasmid DNA occurring together in a single strain. Since sequenced reads are devoted to only a few different sequenced DNA elements (the genome in question or any of its mobile elements), each is expected to be highly covered, and thus for species having low repeat content a good assembly can be achieved.

For natural environments containing many elements, often including those that are difficult to culture [7] in a lab, metagenome assembly is attempted. This technique allows a much broader view of all taxa present and their plasmids, but is limited in that the characterization of each individual element depends on its coverage in the mixed DNA sample and the frequency of co-occurring repeats shared among

different elements of the sample. Resulting assembled genomes of elements that are rare in the environment are thus often fragmented, and very high coverage [8] is needed for accurately assembling them. However, assembly of metagenomes remains a highly active area of research: current assembly outputs are lacking and do not represent the true genetic capacity and synteny of genomes present in complex microbial communities. Since most of the DNA in these environments is due to host genomes, this approach currently provides only limited resolution of plasmids.

Most recently, a third technique has emerged that allows recovery of far greater numbers of plasmids. Plasmidome sequencing [5], [6], [9] allows nearly all sequencing resources to be devoted to circular DNA. Using a protocol described in [5], chromosomal DNA is filtered out and circular DNA segments are selectively amplified. Based on this protocol, hundreds of new plasmids were identified in the cow rumen [6] and rat cecum [9]. In [9], Jørgensen et al. applied the protocol introduced in [5] combined with bioinformatic validation of circularity. This post-assembly analysis resulted in a 95% PCR validation rate out of 40 randomly selected assembled contigs. This success raises the prospect of *in silico* refinement of plasmids beyond the initial assembly. Although Jørgensen et al.'s method was shown to have a high validation rate, its output was highly dependent on the contiguity of the underlying assembler's contigs (in their case IDBA-UD [10]): paths composed of multiple contigs connected at their branch points and contigs shorter than 1000 bp were disregarded. Hence, this method is inherently limited in the proportion of environmental diversity it can detect. To date, no tools for plasmid assembly from short reads have been introduced to address these limitations.

In all of the above approaches plasmid assembly is hindered by several inherent characteristics derived from their mobile nature. These characteristics include their tendency to carry repetitive elements such as insertion sequences and to share genes with other plasmids and microbial genomes. In the context of *de novo* assembly, repeats cause collapse of linear sequences sharing them as subsequences. This creates ambiguity in the sense that it becomes unclear which extensions entering the repeat should be paired with those exiting it, where sequences begin and end, and whether there are unique terminal points at all as opposed to the sequence being circular. *De novo* assembly for the sake of identifying plasmids can be augmented by long-read sequencing [11], [12] because such reads may be sufficiently long to bridge repeats short reads cannot. However, this approach is primarily limited to isolates or low complexity environments. This is evident in that long reads often depend on single molecule sequencing without amplification, thus only capturing relatively abundant DNA fragments. Besides repeats, chimeric sequences also present significant challenges to assembly, in that they create false connections between sequences and thus may lead to misassemblies.

Here, we wish to use more refined analysis in order to improve *de novo* assembly of sequenced plasmids. Our inputs are an assembly graph  $G = (V, E)$ , and the mapping of paired-end reads responsible for the assembly to its nodes. The set of nodes  $V$  are sequences having associated lengths and coverage levels, and the set of arcs  $E$  is composed of directed connections among the nodes. Arcs are the result of branch points in the underlying de Bruijn graph: a branch node has outgoing arcs to two (or more) different nodes based on overlaps, and in many cases the assembler does not have a definite way of choosing which extension is true in order to simplify the branch into a linear path. We aim to generate a set of putative cycles that are likely to be plasmids, and assign a coverage level for each one.

After defining this problem formally below, we present an algorithm (and its implementation) designed to address it, called Recycler. Recycler leverages assembly graphs output by the SPAdes assembler [13] to specifically enable *de novo* assembly of plasmids. We show it greatly improves recovery of plasmids over naive assembly and alternative methods, namely Jørgensen's and SPAdes' built-in repeat resolution, introduced in [14]. We demonstrate Recycler's performance by applying it on both simulated and real data. We find that Recycler greatly increases recall while maintaining high precision. This is established via comparisons performed on simulated plasmidomes of various sizes. We also show that Recycler can be applied for plasmid assembly on real data from a bovine rumen plasmidome and metagenome, and from two different *Escherichia coli* isolate strains. In the isolate cases, Recycler recovered most known plasmids, and predicted additional sequences that matched known mobile

elements from different hosts – all of which were identical or nearly identical to known reference sequences. In all cases on real data, Recycler either matched or exceeded the proportion of outputs matching plasmid annotation, as described in [6].

**Related work** We note plasmid assembly is a multi-assembly problem, as described in the context of RNA-Seq transcriptome assembly [15]. Formulations of such problems often aim to generate a minimal set of paths that maximize agreement with observed data [15]–[17]. These methods usually employ network flow formulations, which admit polynomial-time algorithms for minimizing the cost flow on the network; this flow corresponds to a convex function of the sum of coverage differences between observed and estimated coverage levels. However, these methods resort to heuristics in selecting a minimal set of paths to cover the entire graph, as splitting a flow into a minimal number of path and cycle components is an NP-hard problem [18].

Recycler does not aim to generate a set of paths explaining all coverage levels, and thus does not depend on a global objective function encompassing all nodes or edges. This approach is avoided because of the presence of linear paths due to either plasmids not fully covered during sequencing or bacterial host genomes housing plasmids, which may introduce noise into coverage levels observed and will not be part of the solution. Avoiding a global objective imposing parsimony on paths also allows Recycler to benefit from a polynomial time algorithm for generating 'good' cycles; we prove this property below. Thus, Recycler's approach is similar to StringTie [19], in that both repeatedly seek locally best paths or cycles and use coverage levels estimated on those to update coverage levels on the original graph, until some stopping criterion is met. We note the set of cycles desired is explicitly not minimal, as in cycle cover formulations [20]. For example, given a figure 8 component (Supplementary figure S1, I.) Recycler may represent it as two cycles separated by distinct coverage levels, where a minimal cover would use only one cycle. Instead, we wish to cover as much of the graph as possible with 'good' cycles.

## Methods

**Overview of Recycler** We present the input to our problem as a directed graph with vertices corresponding to non-branching sequence contigs and edges corresponding to connecting overlapping  $k$ -mers. (The graph can be viewed as obtained from the de Bruijn graph of order  $k$  of the sequence data by contracting edges  $(u,v)$  whenever  $u$  has outdegree 1 and  $v$  has indegree 1, and the sequence contig of the new node replacing  $u$  and  $v$  is the concatenation of their sequences). Each node has a coverage value reflecting its abundance in the input sequences. We search for cycles in the graph that will correspond to plasmids. Cycle sequence length, number of vertices, and coverage uniformity are factored in the selection process. We also use paired-end read mappings including mates on different nodes as a proxy for which of the nodes may have emerged from the same physical DNA fragment. This provides a means of inferring whether a candidate cycle is a plasmid or a genomic segment including repeats that lead to ambiguous cycles in the graph. Once a best cycle is selected, its latent coverage level is determined and subtracted from those of all participating nodes. Nodes whose resulting coverage values become non-positive are then removed from the graph, allowing only those with some remaining coverage the opportunity to take part in additional cycles. Hence, the whole process can be viewed as greedily "peeling off" cycles from the graph. Ideally, one would like the process to end in an empty graph, in which case the input graph would be exactly the union of the cycles found. In reality, the process is stopped when quality criteria for new cycles in the remaining graph are unmet.

**Notations and Definitions** Our input is a directed graph  $G = (V,E)$ , where  $V$  is a set of linear sequences having either a branch-point or terminal  $k$ -mer at each end and no internal branch-points.  $E$  is the set of overlaps between nodes, where  $E = \{(u,v): \text{the } (k-1)\text{-mer suffix of } u = \text{the } (k-1)\text{-mer prefix of } v\}$ . We call a node in  $G$  simple if its indegree and outdegree are 1. A node  $v$  corresponding to sequence  $s$  of length  $l(s)$  is assigned two positive values,  $\text{len}(v)$  and  $\text{cov}(v)$ .  $\text{len}(v) = l(s) - k + 1$  is called the *length* of the node (the subtraction is in order avoid double-counting bases common to overlapping segments at their ends).  $\text{cov}(v)$ , its *coverage*, reflects the average number of times each  $k$ -mer in  $s$  appears in the input read data. The input can be produced by a short read assembly tool. We further assign a *weight*

$w(v) = \frac{1}{cov(v)len(v)}$  for each node  $v$ , resulting in low weight for high coverage and long nodes. Longer contigs tend to be less prone to random fluctuations in coverage, and are thus more reliable coverage indicators. For each cycle  $c$  in the graph, we assign each node  $v \in c$  a value  $f(p,v)$  representing its length fraction in  $p$ :  $f(c,v) = \frac{len(v)}{\sum_{\{v \in c\}} len(v)}$ .  $f(p,v)$  is used to define the mean and standard deviation of weighted coverage of cycle  $c$  as  $\mu(c) = \sum_{v \in c} f(c,v)cov(v)$  and  $STD(c) = \sqrt{[\sum_{\{v \in c\}} f(c,v)(cov(v) - \mu(c))^2]}$  respectively, and consequently the coefficient of variation of  $c$ ,  $CV(c) = STD(c)/\mu(c)$ .  $CV(c)$  is used to allow direct comparison of variation levels between cycles, independently of the magnitude of coverage of each.  $CV$  is indicative of coverage uniformity along the cycle, and plasmids are expected to have uniform coverage levels that in many cases are different from other plasmids and their hosts. Thus, a cycle with a lower  $CV$  is more likely to correspond to a plasmid than cycles with higher  $CV$ .

**Our approach** Intuitively, plasmids should form cycles that are distinctive from the rest of the graph and have near uniform coverage. We also expect plasmid cycles to include few nodes, as each additional node introduced for a fixed sequence length increases fragmentation and the tendency of nodes to be common to more than one path. With this in mind, we search for ‘good cycles’ in the graph that potentially correspond to plasmids. Formally, we define a good cycle  $c$  in the graph satisfying the following constraints:

1. **Minimal path weight for some edge:**  $\exists (u,v) \in c$  such that  $c \setminus (u,v)$  (the path obtained by removing  $(u,v)$  from  $c$ ) is a minimum weight path (by sum of weights  $w(v)$ ) from  $v$  to  $u$ .
2. **Low coverage variation:**  $V(c) \leq \tau/|c|$ , where  $\tau$  is a defined threshold and  $|c|$  is the number of nodes in  $c$ .
3. **Concordant read mapping:** For every read pair  $r_1, r_2$ , if  $r_1$  maps to a simple node in  $c$ , then  $r_2$  must also map to some node in  $c$ .
4. **Sufficient sequence length:**  $\sum_{v \in c} len(v) \geq L$ , where  $L$  is a defined threshold.

The first constraint is critical in order to avoid merging of two or more plasmids that are connected through a repeated region (supplementary figure S1, panel I.). Moreover, low weight cycles correspond to longer sequence length and higher coverage nodes, and tend to have fewer nodes. The second constraint ensures that the coverage variation is low, thus again increasing our confidence that the cycle corresponds to exactly one plasmid. Moreover, this constraint implicitly ensures high coverage cycles, since low coverage cycles tend to have higher  $CV$  value. The third constraint exploits paired-end reads. Suppose we have a read pair  $r_1, r_2$  and  $r_1$  maps to a certain node in the candidate cycle  $c$ . We expect  $r_2$  to map to the same cycle, unless  $r_1$  falls on a node that is common to  $c$  and some other path  $p$  overlapping with it. In that case  $r_2$  may map to  $p$  as well. Simple nodes are less likely to overlap with several cycles and path, and the third constraint leverages this observation. We waive this constraint in case the coverage of  $c$  is sufficiently high, as in such cases the cycle "stands out" from the background coverage. See Supplement for details.

The above definition of a good cycle provides a mechanism for the identification of putative plasmids. Recycler processes each strongly connected component separately. It repeatedly finds a good cycle with minimum  $CV$  value, assigns it *latent coverage* equal to the mean cycle coverage and subtracts that coverage from the graph, creating a new *residual coverage* (Figure 1). The weights of the vertices in the cycle are updated based on their new coverage values, and vertices whose resulting coverage values become non-positive are removed from the graph, allowing only those with positive residual coverage the opportunity to take part in additional cycles. After each such change, cycles are recalculated the same way using the updated coverage levels. This process continues as long as new good cycles are found. To avoid examining a potentially exponential number of cycles, we consider one minimum weight cycle through each edge in the graph. Algorithm 1 sketches the procedure for a single component. See the supplement for additional details.

```
Algorithm 1 ( Inputs:  $G = (V, E, len, cov, w)$ ,  $\tau$ ,  $L$  )

Compute shortest cycles passing through each edge:
For each edge (u,v)
    Compute a minimum weight path p from v to u, if one exists
    Compute the CV of the cycle (p,(u,v))
Return the set of cycles S

While  $\Sigma$  changes:
    Compute shortest cycles S
    Consider each cycle c in S in order of increasing CV values
    If c is good and not in  $\Sigma$ 
        Add c to the solution set  $\Sigma$ 
        Compute the latent coverage level of c
        Update the residual coverage of all cycle nodes, removing
        nodes with non-positive residual coverage

Output  $\Sigma$  and end
```

**Complexity** Algorithm 1 presented above terminates in polynomial time. In each iteration, a good cycle is chosen and the mean coverage is calculated. There is at least one node in the cycle with coverage smaller than the mean coverage of the cycle, which is subsequently removed from the graph. Therefore, in each iteration at least one node is removed, and the number of iterations is bounded by the number of nodes. Using Johnson's algorithm [21], the runtime of each iteration is  $O(|V|^2 \log |V| + |V||E|)$ . Running times are further reduced by computing the strongly connected components of  $G$  and working separately on each one.

## **Results**

We first simulated plasmidomes using known references. We used these data sets to assess Recycler's precision and recall (along with those of alternative methods) by comparing predictions against the ground truth known by the simulation design. We also tested Recycler on real data from two E. Coli isolates, and both a cow rumen metagenome and plasmidome [6]. For the bacterial isolates that have been sequenced, predicted plasmids were compared against the reference sequences directly. Since no references are available for metagenome and plasmidome data, we evaluated the accuracy by PCR validation [9] and by measuring the proportion of predicted plasmids having proper annotation as done in [6]. Recycler's inputs were assembly graphs generated by SPAdes version 3.6.2 [13], and alignments generated by BWA version 0.7.5 [22].

**Simulated plasmidomes** We simulated error-free paired-end reads from plasmids using BEAR [23], a read simulator designed to generate artificial metagenome data. To avoid introducing coverage drops at sequence ends typical of linear sequences, we modified BEAR [<https://github.com/rozovr/BEAR>] to allow sampling of reads bridging reference sequence ends, as is observed for circular sequences. Plasmid reference sequences were selected from the NCBI plasmids database and from plasmid sequences reported in [6], filtered to include 2760 sequences with a length range of 1 to 20 kbp with a mean of 6337 bp. Five datasets were created, composed of 100 bp mates (read pair ends), with insert sizes  $\sim N(500,100)$ , varying from 1.25M pairs sampled on 100 reference sequences doubling successively up to 20M pairs sampled on 1600 sequences. Abundance levels were assigned using BEAR's low complexity option, which concentrates high abundance to few species using a power function with parameters derived from [24]: the function takes the form  $ci^d$ , where  $c=31.4$  and  $d=-1.28$ , and  $i$  is iteratively assigned values from 1 to the number of species simulated. These values are then normalized by their sum to yield a probability distribution.

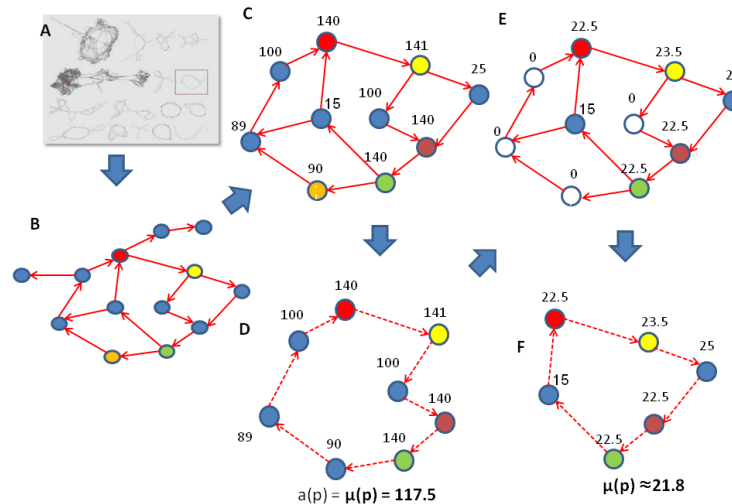


**Figure 1** Recycler work-flow. A. The assembly graph. B. A single component is selected from the assembly graph (framed in A) and represented with vertices for contigs and edges for connecting k-mers. C. The reduced component after tip removal. Vertex values are observed contig coverage. For simplicity, all lengths are assumed to be equal and not shown. D.-F. Two successive peelings of cycles are shown with their respective latent coverage assignments.

Each such dataset was assembled with SPAdes and subsequently its output contigs and assembly graphs were used as inputs to other methods. To test recovery of the ground truth sequences, we used the Nucmer alignment tool [25], which is designed for efficiently comparing long nucleotide sequences such as those of whole plasmids or chromosomes. In order to simplify this process, we modified reference sequences to remove non-ACGT characters before read simulation and alignments. To avoid fragmented alignments caused by differences in start positions, we concatenated each reference sequence to itself before mapping; this allowed identification of complete matches at the center of the concatenated contigs when they were present. Recycler was compared with SPAdes with and without repeat resolution, and to a simplified version of Jørgensen’s method (described in the appendix). We used SPAdes’ outputs before the repeat resolution stage as inputs to Recycler and to a Jørgensen’s method, as we found that contigs have greater precision before RR when compared to reference sequences (as shown in supplementary Table 1). The mapping results are presented in supplementary Table 1 and Figure 2. Output cycles were defined as true positives (TP) if they had 100% identity hits covering at least 80% of one of the reference sequences. False positives (FP) were any output cycles not meeting these criteria, and false negatives (FN) were reference sequences not aligned to in the output set using these criteria. Based on these conventions,  $precision = \frac{TP}{TP+FP}$  and  $recall = \frac{TP}{TP+FN}$ . We used the score  $F1 = \frac{2*precision*recall}{precision+recall}$  [26] to combine these measures in a manner that weighs precision and recall equally.

As expected, recall generally decreased as the number of simulated plasmids increased. This was common to all tested methods. In general, we found that Recycler generated more predictions than other methods, leading it to have higher recall than alternative approaches while maintaining high (~90%) precision. The net performance effect is shown in Figure 2: Recycler maintains the lead in all cases with 5-14% F1 advantage. We also found that number of additional Recycler the true positives over those provided by SPAdes increased with higher complexity; this culminated in Recycler adding 13% true positives to SPAdes’ output on the 1600 plasmid set (523 vs. 461).

To further characterize Recycler’s performance, we categorized its predictions in terms of mean total cycle length, number of segments in the cycle (“steps”), cycle coverage, and CV value calculated at the stage the cycle was removed. For each category, values were subdivided into five ranges. In Figure 3, we show the precision values and the relative proportions of counts in the specified ranges. Based on this stratification, it can be seen in Figure 3 that Recycler shows little dependence on mean coverage or

length, but does often preclude candidate cycles that have high CV values or number of steps. This is reflected in the sharp drop-off in the plots as the number of steps or the CV grows.

### **Real data**

All of Recycler's results on real data were subjected to quantification of annotation results as described in [6] and compared against cycles present in the output produced by SPAdes. These results are detailed below and a summary of them can be found in Table S2 in the Appendix.

**E. Coli isolate data** We ran Recycler on two E. Coli strains: JJ1886, downloaded from <http://www.ebi.ac.uk/ena/data/view/SRX321704>, and E2022, sequenced locally. Annotation for plasmids found in both strains was provided in [27]; their lengths are reported in Supplementary Tables 3 and 4. Of the five plasmids known for JJ1886, Recycler output four complete matches (100% identity over 100% length) having lengths 55.9, 5.6, 5.2, and 1.6 kbp. It also output three additional sequences which completely matched previously reported plasmids: two are known to be present in Staph. aureus, and one in Staph. chromogenes. Further tests will be needed in order to validate whether these additional hits are truly present in the sequenced sample, and furthermore, whether they are stable residents of the tested hosts or were present as a result of contamination. When tested on E2022, Recycler performed similarly, recalling most of its known plasmids and outputting a few additional cycles that were complete or near complete matches to known plasmids and one phage. These results are also presented in Supplementary Table 2. In summary, all reported isolate hits represent highly accurate matches to known mobile elements, and most known plasmids for these strains were recovered. In both cases Recycler missed the longest known reference plasmids; it remains to be seen whether this is due to Recycler's use of a shortest path formulation, lack of significant coverage difference between these plasmids and the host genome, or other factors.

**Plasmidomes and PCR validation results** A bovine rumen plasmidome sample was prepared as described in [6]. This data consisted of 5.1 M paired-end 101 bp reads (trimmed to varied sizes for the sake of adapter removal) with an expected insert size of 500 bp [data available upon request]. Recycler output 420 cycles when provided this data. According to ORF prediction performed as in [6], 314 of the 420 had significant annotation hits. 96% of those matching annotations either matched plasmid annotations or aligned with plasmids reported in [9]. Thus, a majority are likely to be plasmids. In addition, out of 8 known plasmids previously validated by PCR (produced by the 2-step assembly procedure described in the appendix), 6 were fully recovered in Recycler's output.

**Metagenome data** Metagenome data was derived from the rumen of a different cow residing in the same stable as the cow used to derive the plasmidome data. This data consisted of 7.5 M paired end 150 bp reads with expected insert size of 500 bp [data available upon request]. Recycler produced 40 cycles when run on this data. According to ORF prediction, 37 of the 40 had significant annotation hits. 35% of those matching annotations either matched plasmid annotations or aligned with plasmids reported in [9]. The proportion of reported cycles matching known plasmid annotations was slightly higher than for simple cycles output by SPAdes (33%). Overall, this test reflects the trend seen elsewhere [8] of weak annotation results emerging from metagenome assembly of highly diverse environmental samples.

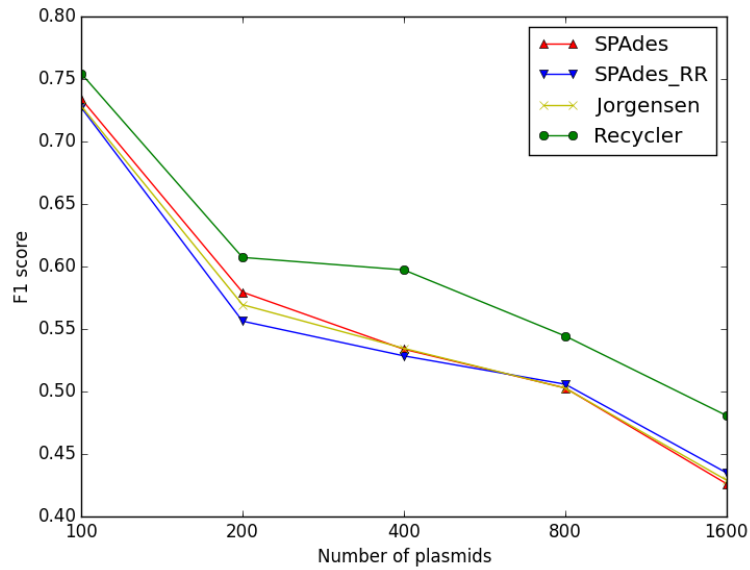


**Figure 2** Methods performance on simulated data. Results are shown for SPAdes without repeat resolution (RR), SPAdes with repeat resolution, the method of Jørgensen et al, and Recycler. The contigs of SPAdes before RR were used as input for the three other methods. Recycler also relied on the graph produced at this stage. F1 score calculation is described in the main text. The x axis shows the number of simulated reference sequences in each case.

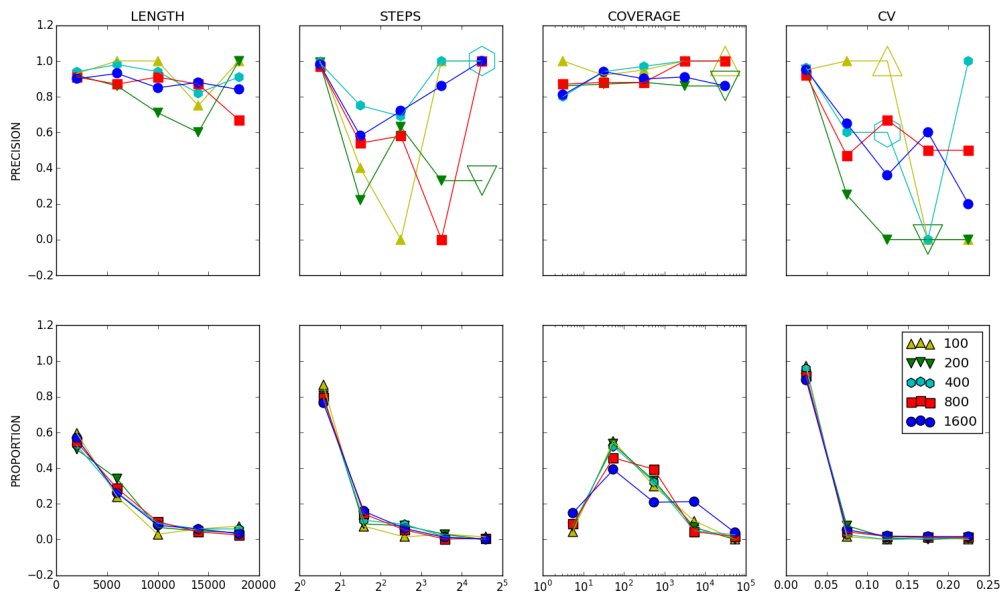


**Figure 3** Recycler's precision, stratified by different properties. TOP: For simulated reads, true positive (100% identity over 80% reference length) alignment proportions were tallied inside 5 bins corresponding to value ranges of different properties - total assembly length (LENGTH), number of nodes in the cycle (STEPS), mean coverage level on the paths (COVERAGE), and cycle coefficient of variation (CV). Each point represents the precision rate for all simulated plasmids included in that range in the specified reference set. Reference sets are denoted by different colors and marker shapes. Enlarged empty markers are used to indicate the absence of any instances having the given property & bin combination. BOTTOM: relative proportions of counts inside each bin out of all outputs.

## Discussion

In this article, we describe Recycler, a new algorithm and the first tool available for identification of plasmids from short read-length deep sequencing data. We demonstrate that Recycler discovers plasmids that remain fragmented after de novo assembly. We have adapted the approach of choosing among likely enumerated paths using coverage and length properties, (often applied in transcriptome assembly, e.g., [16], [19], [17]) for extracting a specific but common inhabitant of metagenomes. We



showed that many more real plasmids can be found by only generating likely cycles on the assembly graph versus alternative methods. We validated this approach on both real and simulated data.

Recycler displays high recall and precision on simulated plasmidomes, and we have developed a means of separating real plasmids from cycles due to repeats in isolate data. As we have noted, coverage can be very useful for the latter, but the assumption that coverage will always differ significantly between plasmids and their host genome does not hold universally. It is worth noting that as new plasmids are identified and their common sequence motifs are observed, both reference-based identification and a priori trained prediction of plasmid features can be improved and harnessed for supplementing identification based on coverage and length features alone. We aim to investigate how such knowledge can be leveraged for increased precision without sacrificing recall.

Further investigation will be needed to assess how plasmids can be extracted from environmental samples, in spite of the limitations now hampering metagenome assembly. Currently, a ‘Catch-22’ situation persists, in that diverse genomes require very high coverage for rare species to be captured, but such high coverage data demand computational resources beyond reach of most investigators in order to obtain high quality assemblies. While new techniques have aimed to address this problem [8], [28], they have yet to see widespread use, and work best when paired with multiple samples to allow for species separation by co-abundance signatures. Along with addressing these concerns, it remains to be seen whether a mixed approach of pre-screening environmental samples for plasmids and computationally filtering them out may benefit metagenome graph simplification.

### **Acknowledgements**

Research partially supported by the Israel Science Foundation grants no. 1425/13 (EH), 317/13 (RS), 1313/13 (IM) and the ISF-NSFC joint program 2015-18 (RS). Additional support was provided by the European Research Council (ERC) under the European Union’s Horizon 2020 research and innovation program (grant agreement No 640384, IM). RR was supported in part by a fellowship from the Edmond J. Safra Center for Bioinformatics at Tel Aviv University, an IBM PhD fellowship, and by the Center for Absorption in Science, the Israel Ministry of Immigrant Absorption. EH is a Faculty Fellow of the Edmond J. Safra Center for Bioinformatics at Tel Aviv University. RR wishes to thank Kobi Perl and David Pellow for helpful comments given in the preparation of the manuscript.

### **Bibliography**

- [1] H. P. Doring and P. Starlinger, “Barbara McClintock’s controlling elements: now at the DNA level,” *Cell*, vol. 39, pp. 253–259, 1984.
- [2] S. Halary, J. W. Leigh, B. Cheaib, P. Lopez, and E. Bapteste, “Network analyses structure genetic diversity in independent genetic worlds,” *Proc. Natl. Acad. Sci.*, vol. 107, no. 1, pp. 127–132, Dec. 2009.
- [3] H. C. Neu, “The Crisis in Antibiotic Resistance,” *Science (80-. )*, vol. 257, no. 5073, pp. 1064–1073, Aug. 1992.
- [4] C. M. Bevan MW, Flavell RB, “A chimaeric antibiotic resistance gene as a selectable marker for plant cell transformation,” *Nature*, no. 304, pp. 184–187, 1983.
- [5] A. Brown Kav, I. Benhar, and I. Mizrahi, “A method for purifying high quality and high yield plasmid DNA for metagenomic and deep sequencing approaches,” *J. Microbiol. Methods*, vol. 95, no. 2, pp. 272–9, Nov. 2013.
- [6] A. Brown Kav, G. Sasson, E. Jami, A. Doron-Faigenboim, I. Benhar, and I. Mizrahi, “Insights into the bovine rumen plasmidome,” *Proc. Natl. Acad. Sci. U. S. A.*, vol. 109, no. 14, pp. 5452–7, Apr. 2012.
- [7] J. A. Gilbert and C. L. Dupont, “Microbial metagenomics: beyond the genome,” *Ann. Rev. Mar. Sci.*, vol. 3, pp. 347–71, Jan. 2011.
- [8] A. C. Howe, J. K. Jansson, S. A. Malfatti, S. G. Tringe, J. M. Tiedje, and C. T. Brown, “Tackling soil diversity with the assembly of large, complex metagenomes,” *Proc. Natl. Acad. Sci. U. S. A.*, vol. 111, no. 13, pp. 4904–9, Apr. 2014.
- [9] T. S. Jørgensen, Z. Xu, M. A. Hansen, S. J. Sørensen, and L. H. Hansen, “Hundreds of circular novel plasmids and DNA elements identified in a rat cecum metamobilome,” *PLoS One*, vol. 9, no. 2, p. e87924, Jan. 2014.
- [10] Y. Peng, H. C. M. Leung, S. M. Yiu, and F. Y. L. Chin, “IDBA-UD: a de novo assembler for single-cell and metagenomic sequencing data with highly uneven depth,” *Bioinformatics*, vol. 28, no. 11, pp.

- 1420–8, Jun. 2012.
- [11] S. Conlan, P. J. Thomas, C. Deming, M. Park, A. F. Lau, J. P. Dekker, E. S. Snitkin, T. A. Clark, K. Luong, Y. Song, Y.-C. Tsai, M. Boitano, J. Dayal, S. Y. Brooks, B. Schmidt, A. C. Young, J. W. Thomas, G. G. Bouffard, R. W. Blakesley, J. C. Mullikin, J. Korlach, D. K. Henderson, K. M. Frank, T. N. Palmore, and J. A. Segre, “Single-molecule sequencing to track plasmid diversity of hospital-associated carbapenemase-producing Enterobacteriaceae,” *Sci. Transl. Med.*, vol. 6, no. 254, p. 254ra126, Sep. 2014.
- [12] M. Hunt, N. De Silva, T. D. Otto, J. Parkhill, J. A. Keane, and S. R. Harris, “Circlator: automated circularization of genome assemblies using long sequencing reads,” *Cold Spring Harbor Labs Journals*, Jul. 2015.
- [13] A. Bankevich, S. Nurk, D. Antipov, A. A. Gurevich, M. Dvorkin, A. S. Kulikov, V. M. Lesin, S. I. Nikolenko, S. Pham, A. D. Prjibelski, A. V Pyshkin, A. V Sirotkin, N. Vyahhi, G. Tesler, M. A. Alekseyev, and P. A. Pevzner, “SPAdes: a new genome assembly algorithm and its applications to single-cell sequencing,” *J. Comput. Biol.*, vol. 19, no. 5, pp. 455–77, May 2012.
- [14] A. D. Prjibelski, I. Vasilinets, A. Bankevich, A. Gurevich, T. Krivosheeva, S. Nurk, S. Pham, A. Korobeynikov, A. Lapidus, and P. A. Pevzner, “ExSPAnDer: a universal repeat resolver for DNA fragment assembly,” *Bioinformatics*, vol. 30, no. 12, pp. i293–301, Jun. 2014.
- [15] V. Mäkinen, D. Belazzougui, F. Cunial, and A. I. Tomescu, *Genome-Scale Algorithm Design*. Cambridge University Press, 2015.
- [16] A. I. Tomescu, A. Kuosmanen, R. Rizzi, and V. Mäkinen, “A novel min-cost flow method for estimating transcript expression with RNA-Seq,” *BMC Bioinformatics*, vol. 14 Suppl 5, no. 5, p. S15, Jan. 2013.
- [17] C. Trapnell, B. A. Williams, G. Pertea, A. Mortazavi, G. Kwan, M. J. van Baren, S. L. Salzberg, B. J. Wold, and L. Pachter, “Transcript assembly and quantification by RNA-Seq reveals unannotated transcripts and isoform switching during cell differentiation,” *Nat. Biotechnol.*, vol. 28, no. 5, pp. 511–5, May 2010.
- [18] T. Hartman, A. Hassidim, H. Kaplan, D. Raz, and M. Segalov, “How to split a flow?,” in *2012 Proceedings IEEE INFOCOM*, 2012, pp. 828–836.
- [19] M. Pertea, G. M. Pertea, C. M. Antonescu, T.-C. Chang, J. T. Mendell, and S. L. Salzberg, “StringTie enables improved reconstruction of a transcriptome from RNA-seq reads,” *Nat. Biotechnol.*, vol. 33, no. 3, pp. 290–295, Feb. 2015.
- [20] *Handbook of Graph Theory*. CRC Press, 2004.
- [21] D. B. Johnson, “Efficient Algorithms for Shortest Paths in Sparse Networks,” *J. ACM*, vol. 24, no. 1, pp. 1–13, Jan. 1977.
- [22] H. Li and R. Durbin, “Fast and accurate short read alignment with Burrows-Wheeler transform,” *Bioinformatics*, vol. 25, no. 14, pp. 1754–60, Jul. 2009.
- [23] S. Johnson, B. Trost, J. R. Long, V. Pittet, and A. Kusalik, “A better sequence-read simulator program for metagenomics,” *BMC Bioinformatics*, vol. 15 Suppl 9, no. Suppl 9, p. S14, Jan. 2014.
- [24] M. Pignatelli and A. Moya, “Evaluating the fidelity of de novo short read metagenomic assembly using simulated data,” *PLoS One*, vol. 6, no. 5, p. e19984, Jan. 2011.
- [25] S. Kurtz, A. Phillippy, A. L. Delcher, M. Smoot, M. Shumway, C. Antonescu, and S. L. Salzberg, “Versatile and open software for comparing large genomes,” *Genome Biol.*, vol. 5, no. 2, p. R12, Jan. 2004.
- [26] D. Powers, “Evaluation: From Precision, Recall and F Factor to ROC, Informedness, Markedness & Correlation,” *Sch. Informatics Eng. Flinders ...*, 2007.
- [27] V. F. Lanza, M. de Toro, M. P. Garcillán-Barcia, A. Mora, J. Blanco, T. M. Coque, and F. de la Cruz, “Plasmid flux in Escherichia coli ST131 sublineages, analyzed by plasmid constellation network (PLACNET), a new method for plasmid reconstruction from whole genome sequences,” *PLoS Genet.*, vol. 10, no. 12, p. e1004766, Dec. 2014.
- [28] B. Cleary, I. L. Brito, K. Huang, D. Gevers, T. Shea, S. Young, and E. J. Alm, “Detection of low-abundance bacterial strains in metagenomic datasets by eigengenome partitioning,” *Nat. Biotechnol.*, vol. 33, no. 10, pp. 1053–1060, Sep. 2015.

## Appendix

| No. Reference Plasmids | SPAdes cycles before RR | SPAdes TPs before RR | SPAdes cycles after RR | SPAdes TPs after RR | Jørgensen cycles | Jørgensen TPs | Recycler cycles | Recycler TPs | No. added, % |
|------------------------|-------------------------|----------------------|------------------------|---------------------|------------------|---------------|-----------------|--------------|--------------|
| 100                    | 58                      | 58                   | 65                     | 60                  | 62               | 59            | 67              | 63           | 3, 5         |
| 200                    | 83                      | 82                   | 102                    | 84                  | 88               | 82            | 103             | 92           | 8, 9.5       |
| 400                    | 147                     | 146                  | 171                    | 153                 | 165              | 151           | 186             | 175          | 22, 14       |
| 800                    | 274                     | 270                  | 319                    | 283                 | 322              | 282           | 350             | 313          | 30, 10.6     |
| 1600                   | 437                     | 434                  | 520                    | 461                 | 498              | 450           | 576             | 523          | 62, 13.4     |

**Table 1** Counts of output cycles vs. true positives (TPs) for each method. The number of reference plasmids reflects the number of sequences that were simulated. The number of cycles reflects the total output by each method, and the true positives represent those that match some reference sequence based on alignment criteria defined in the main text. The last column shows Recycler's advantage over SPAdes with repeat resolution in number of plasmids and percentage added.

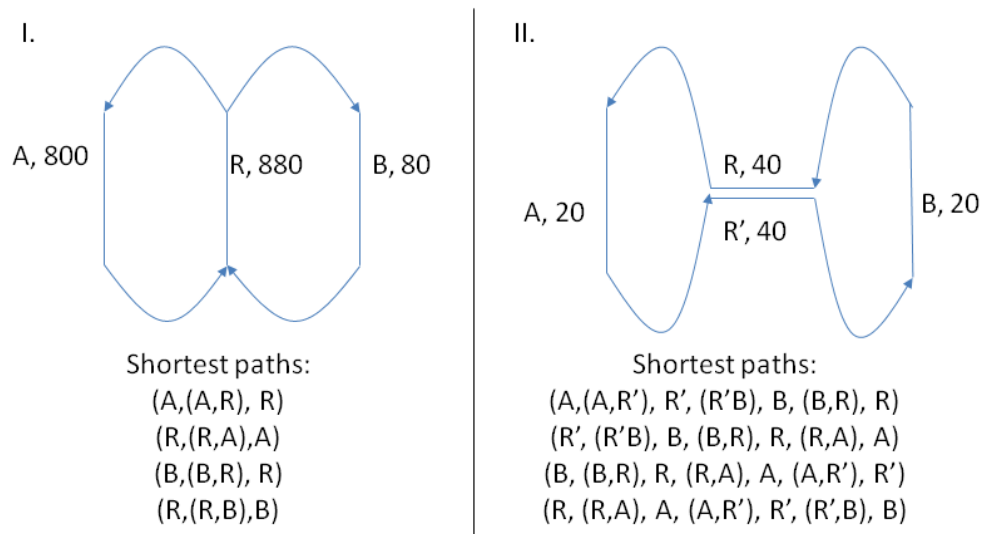


**Figure S1** Shortest paths through repeats. Nodes are represented as lines, and edges as arrows. For each node  $x$ ,  $x'$  represents its reverse complement node. All node lengths are 1. I.) Recycler will consider only the shortest paths shown as candidates. The shortest path criterion described in the Methods section allows Recycler to avoid looping in a path with the shape “figure 8.” II.) For the component on the right, Recycler must consider shortest paths including the figure 8 path covering the entire component, as R and R' have different adjacencies. In such cases, Recycler will assign equal parts of the coverage to R and R': each gets 20. This demonstrates the use of the shortest path criteria in only allowing repeated traversal of nodes when warranted by coverage and orientation.

### 2-step assembly procedure

We tested another assembly strategy, which we call 2-step assembly. That procedure used the ability of SPAdes to use libraries of different insert lengths. Reads were first assembled using SPAdes, then aligned to the assembled contigs using BWA [19], then split into groups (based on alignment properties) which were treated as separate sequenced libraries on which a second round of SPAdes assembly was performed. The splitting of reads was based on BAM file alignment property flags. These flags separated read pairs into ‘proper’ pairs -- those having correct orientation and expected insert size --

and improper pairs that fail to meet at least one of these criteria. These two read groups were used as separate inputs to a second execution of SPAdes, with the aim of benefitting from improved repeat resolution and formation of more cycles. The last step of this procedure re-examined mapping of read pairs, this time focusing on contig ends. The purpose of this step was the identification of self-loops closed by read pairs where these loops did not close in the assembly graph.

We tested the effect of the 2-step procedure on the performance of Recycler using the 1600 reference simulated data set. We assessed the number of cycles generated with and without second steps and application of Recycler. Far fewer cycles were obtained with the 2-step assembly, implying a strong reduction in recall by virtue of the number of candidates alone.

|                 | SPAdes cycles before RR | Recycle cycles |
|-----------------|-------------------------|----------------|
| 1 step assembly | 437                     | 576            |
| 2 step assembly | 340                     | 370            |

### **Jørgensen's method**

We only used the first part of the protocol described Jørgensen's method in order to allow for maximal recall; the second part involved further filtering (and thus reduction) of the first part's results. Circular contigs were identified by finding those having opposite ends that overlap. These were then refined by breaking those that do have such overlaps into halves, and then gluing the far ends by applying the minimus2 assembler, part of the AMOS package.

**Table 2 – Real data results summary**

|                                      | E2022<br>Recycler | E2022<br>SPAdes | JJ1886<br>Recycler | JJ1886<br>SPAdes | metagenome<br>Recycler | metagenome<br>SPAdes | plasmidome<br>Recycler | plasmidome<br>SPAdes |
|--------------------------------------|-------------------|-----------------|--------------------|------------------|------------------------|----------------------|------------------------|----------------------|
| No. seqs annotated as plasmids       | 5                 | 3               | 7                  | 3                | 12                     | 10                   | 249                    | 203                  |
| No. seqs with hits on [9] data       | 0                 | 0               | 0                  | 0                | 1                      | 0                    | 53                     | 50                   |
| No. seqs with any nr annotation      | 5                 | 3               | 7                  | 3                | 37                     | 30                   | 314                    | 264                  |
| total No. cyles                      | 5                 | 3               | 7                  | 3                | 40                     | 33                   | 420                    | 361                  |
| % annotated cyles as plasmids        | 100               | 100             | 100                | 100              | 32                     | 33                   | 79                     | 77                   |
| % annotated cyles as plasmids or [9] | 100               | 100             | 100                | 100              | 35                     | 33                   | 96                     | 96                   |
| % annotated at all                   | 100               | 100             | 100                | 100              | 93                     | 91                   | 75                     | 73                   |

**Table 3 – plasmids detected by Recycler on E.Coli strain E2022**

| Ref. length (Kb) | Output length (Kb) | Top blast hit | ID (%) | Len. (%) |
|------------------|--------------------|---------------|--------|----------|
|------------------|--------------------|---------------|--------|----------|

|      |      |                               |     |     |
|------|------|-------------------------------|-----|-----|
|      | 1.5  | E. Coli FHI63 plasmid         | 100 | 100 |
| 2.2  | 2.1  | E. coli GXEC6 plasmid         | 100 | 100 |
| 4.1  | 4.1  | Jørgensen et al. plasmid      | 100 | 99  |
|      | 5.4  | Enterobacteria phage phi-x174 | 100 | 100 |
| 35   | 33.1 | E coli GXEC6 plasmid          | 97  | 99  |
| 98.3 |      |                               |     |     |
| 103  |      |                               |     |     |

**Table 4 - plasmids detected by Recycler on E.Coli strain JJ1886**

| Ref. length (Kb) | Output length (Kb) | Top blast hit              | ID (%) | Len. (%) |
|------------------|--------------------|----------------------------|--------|----------|
| 1.6              | 1.6                | JJ1886 plasmid             | 100    | 100      |
|                  | 1.6                | staph. aureus plasmid      | 100    | 100      |
|                  | 2.2                | staph. aureus plasmid      | 100    | 100      |
|                  | 2.4                | staph. chromogenes plasmid | 100    | 100      |
| 5.2              | 5.2                | JJ1886 plasmid             | 100    | 100      |
| 5.6              | 5.6                | JJ1886 plasmid             | 100    | 100      |
| 56.0             | 56.0               |                            |        |          |
| 103              |                    |                            |        |          |

### Algorithm details

**Definitions, notation** For all  $v \in V, w_i(v) = \frac{1}{len(v)cov_i(v)}$ . These are used to find minimal cost paths in calls to Johnson's [21] algorithm. When applying Johnson's algorithm, each edge (u,v) is assigned weight w(u), as Johnson's algorithm depends on edge weights instead of node weights to calculate minimum cost paths. Each time a cycle p is peeled from a component, coverage levels are updated to be  $cov_{i+1} = \max(cov_i - \mu(p), 0)$  for all nodes in p.

$$len(p) = \sum_{\{v \in p\}} len(v)$$

$|p|$  = the number of contigs in p

**thresh** is set to the 75<sup>th</sup> percentile of simple node coverage levels for plasmidome data sets, and the 95<sup>th</sup> percentile for isolate data sets. This threshold is used in the testing for good paths. We use a different threshold for the two scenarios as it is easier to distinguish between coverage levels typical for the genome vs. foreign elements on isolate data than it is for more diverse environmental samples.

#### **'Good' path conditions:**

- $len(p) \geq \ell_{\{min\}}$
- $CV(p) \leq \frac{\tau}{|p|}$
- CASE\_A: All reads  $r_{i1}$  mapping to simple nodes in path p have their mates  $r_{i2}$  mapping to some  $v_i$  such that  $v_i$  is on p
- CASE\_B:  $\mu(\text{path}) \geq \text{thresh}$

Define  $(r_i, v_i)$  as an alignment of read  $r_i$  to  $v_i$ . Then the set of paired-end reads with mates aligned to different contigs is denoted as  $A_{GR} = \{(r_1, v_1), (r_2, v_2): r_1 = \text{mate}(r_2), v_1, v_2 \in V, v_1 \neq v_2\}$

Define SCC(G) to be the set of strongly connected components of G

**Algorithm:**

**Inputs:**  $G = (V, E)$ ,  $\tau$ ,  $\ell_{min}$ ,  $A_{GR}$

```

func recycle(G,  $A_{GR}$ ,  $\tau$ ,  $\ell_{min}$ ):
    cycles = {(u,u) : u ∈ V is a simple node}
    for COMP in SCC(G):
        cycles = cycles U peel_cycles(COMP,  $A_{GR}$ ,  $\tau$ ,  $\ell_{min}$ )
    return cycles

func peel_cycles(COMP,  $A_{GR}$ ):
    paths = get_shortest_pred_paths(COMP)
    last_path_count = 0
    last_node_count = 0
    while(|final_paths| ≠ last_path_count OR |VCOMP| ≠ last_node_count):
        last_node_count = |VCOMP|
        last_path_count = |final_paths|
        paths = sort_by_CV(paths)
        curr_path = paths.pop() # get lowest CV path
        if is_good_path(curr_path,  $A_{GR}$ , ) and curr_path ∉ final_paths:
            update_path_coverage_vals(curr_path, COMP)
            final_paths = final_paths U {curr_path}
        paths = get_shortest_pred_paths(COMP)
    return final_paths

func get_shortest_pred_paths(comp):
    paths = {}
    shortest_paths = Johnson(G,W)
    for v in Vcomp:
        preds = {u: (u,v) ∈ Ecomp}
        (path, path_cost) = shortest_paths(v,u)
        if path_cost < ∞:
            paths = paths U {path}
    return paths

func is_good_path(path,  $A_{GR}$ ):
    if (len(path) ≥  $\ell_{min}$ ) AND ( (IS_CASE_A(path)) OR (IS_CASE_B(PATH,  $A_{GR}$ )) ):
        return TRUE
    else:
        return FALSE

func update_path_coverage_vals(path, G):
    μ = weighted_mean_coverage(path)
    for v in path:
        cov(v,G) = cov(v,G) - μ
        if cov(v,G) ≤ 0:
            remove(v,G)

```